Video Article

In Vivo Morphometric Analysis of Human Cranial Nerves Using Magnetic Resonance Imaging in Menière's Disease Ears and Normal Hearing Ears

Wilhelm H. Flatz[1], Annika Henneberger[2], Maximilian F. Reiser[1], Robert Gürkov[3], Birgit Ertl-Wagner[1]

[1]Department of Radiology, University Hospital, LMU Munich

[2]Department of Otorhinolaryngology - Head and Neck Surgery, SLK-Kliniken Heilbronn GmbH

[3]Department of Otorhinolaryngology Head and Neck Surgery, Ludwig-Maximilians-University Hospital Munich, German Centre for Vertigo and Balance Disorder

Correspondence to: Wilhelm H. Flatz at wflatz@med.uni-muenchen.de

URL: https://www.jove.com/video/57091
DOI: doi:10.3791/57091

Keywords: Medicine, Issue 132, Morphometry, MRI, cranial nerves, cross-sectional area, facial nerve, vestibulocochlear nerve, endolymphatic hydrops, cranial nerve VII, cranial nerve VIII, 7th cranial nerve, 8th cranial nerve

Date Published: 2/21/2018

Citation: Flatz, W.H., Henneberger, A., Reiser, M.F., Gürkov, R., Ertl-Wagner, B. *In Vivo* Morphometric Analysis of Human Cranial Nerves Using Magnetic Resonance Imaging in Menière's Disease Ears and Normal Hearing Ears. *J. Vis. Exp.* (132), e57091, doi:10.3791/57091 (2018).

Abstract

Analysis of neural structures in Menière's Disease (MD) is of importance, since a loss of such structures has previously been proposed for this patient group but has yet to be confirmed. This protocol describes a method of *in vivo* evaluation of neural changes especially well suitable for cranial nerve analysis using magnetic resonance imaging (MRI). MD-patients and normal hearing persons were examined in a 3-T MR-scanner using a scan protocol including strongly T2-weighted 3D gradient-echo-sequence (3D-CISS). In the patient group, MD was additionally confirmed using MRI-based assessment of endolymphatic hydrops. Morphometric analysis was performed using a freeware DICOM viewer. Evaluation of cranial nerves included measurements of cross-sectional areas (CSAs) of the nerves at different levels as well as orthogonal diametric measurements.

Video Link

The video component of this article can be found at https://www.jove.com/video/57091/

Introduction

Magnetic resonance imaging (MRI) plays a major role in visualizing and analyzing anatomy as well as physiological and pathological processes in the human body. Since clinical and electrophysiological diagnosis of Menière's Disease (MD) can be challenging, using additional information derived from MRI is more than helpful[1,2,3,4]. An *in vivo* method was developed to analyze endolymphatic hydrops in MD and morphometric changes of cranial nerves using MRI. With this combined approach, diagnosis of definite MD was confirmed, and morphometric changes of cranial nerves were studied at different levels throughout the course of the nerves. Etiology of MD is still unclear[5,6,7]. It was proposed that neural cell loss could be involved in MD, but this has yet to be confirmed.

Suitable cranial nerves for morphometric analysis in MD are the 7th and 8th nerve with its branches, which were analyzed in this study. Only a few studies can be found analyzing morphometric aspects of these nerves using MRI[8,9,10]. The study by Henneberger *et al.* analyzed morphometric changes of the 7th and 8th cranial nerve in MD ears compared to normal hearing ears[11].

The method presented here enables *in vivo* visualization and morphometric analysis of the 7th and 8th cranial nerves throughout their course from the brain to the temporal bone. Using this method, we have shown that there are significant differences between the patient group of MD patients and healthy ears. We propose the described method for use in several situations/diseases whenever potential morphometric changes of cranial nerves are of interest. Whether this method will be established in clinical diagnostic workups remains to be evaluated by future studies. Real alternatives to the described method for *in vivo* evaluation of morphometric changes of cranial nerves are not available, and while computed tomography (CT) has its strengths such as wide availability, speed, and depiction of bony changes, it also exhibits too low tissue contrasts to visualize subtle changes in cranial nerves within the neurocranium and temporal bone. *Post mortem* analysis of cranial nerve changes in MD patients remains to be studied. With special imaging and evaluation techniques as described here, it is possible to analyze morphometric changes of cranial nerves in MD patients and healthy controls using MRI. Routine MRI workup of the brain often does not include high resolution, strongly T2-weighted imaging techniques, which are mandatory for the evaluation of morphometric changes of cranial nerves 7 and 8.

The developed method may have further diagnostic impact on evaluating different levels of severity in MD, as well as play a role in the evaluation of vertigo, hearing deficits, and tinnitus. Specialized centers for diagnostic and therapeutic workup of vertigo play a major role in today's health care systems and our method could provide specialists with a possible tool for their diagnostic workup[12,13,14]. Vertigo is a complex symptom occurring in several diseases, requiring a thorough interdisciplinary cooperation between different specialties, as demonstrated in specialized centers for diagnostic and therapeutic workup of vertigo[12,13,14].

To our knowledge, there is no method available in the literature for *in vivo* morphometric analysis of cranial nerves in MD and healthy controls.

Protocol

All the procedures were approved by the local ethical committee (Institutional review board of the University of Munich/LMU Munich Protocol No. 093-09). All patients gave their informed consent to the performed procedures.

1. Clinical Examination

1. Identify patients suffering from suspected MD in cooperation with the Department for Ear, Nose and Throat (ENT).
    1. Perform clinical evaluation; vertigo, tinnitus/ringing of the ear, and hearing loss (possibly fluctuating) need to be evaluated. Check for associated nausea and vomiting. Check for the duration of the symptoms.
    2. Take the clinical and functional test results into consideration for diagnosis of MD: check for the results of audiometry, caloric video-oculography, vestibular evoked myogenic potentials (VEMP), and electrocochleography (ECoG) in the hospital papers or electronic medical record system.
    3. Check for typical findings in MD: audiometry may show impaired hearing levels in pure tone averaging (PTA), caloric irrigation can reveal horizontal semicircular paresis, SP/AP ratio may be pathologically high in ECoG, and VEMP interaural amplitude ratio may be significantly lower in MD patients.

2. MRI Image Acquisition in Patients Suffering from MD and Healthy Controls

1. Apply an intratympanic gadolinium-injection 24 h prior to the MRI scan in the patient group. Inject 0.4 mL of a gadolinium-based contrast agent intratympanically, (*e.g.*, Magnograf diluted 8-fold in saline), 24 h prior to the scheduled MRI-scan.
2. Prepare the patient for MRI examination: check for metal implants (exams are feasible with a pacemaker if adequate precautions are taken; dental implants are usually feasible), claustrophobia, *etc.* Use noise reduction devices such as noise reduction headphones for protection of patient hearing.
3. Position the patient adequately into the scanner. Position the patient's head straight, and fit and close the MR-head coil. Position the patient's head/temporal bone at the isocenter of the MR scanner.
4. Perform the MRI-scan according to the study protocol, including 3D-FLAIR- and 3D-real IR-sequences for detection of endolymphatic hydrops in the patient group and strongly T2-weighted 3D-CISS for morphologic analysis of cranial nerves in the patient group and healthy controls.
5. Set the sequence parameters for the morphometric scan 3D-CISS as follows: repetition time (TR) 5.79 ms, echo time (TE) 2.58 ms, flip angle 34°, field of view (FoV) 160 x 160 mm^2, matrix size 320 x 320, number of averages 1, slice thickness 0.5 mm (**Table 1**). Perform the scans of the 3D-FLAIR using a TR of 9,000 ms, TE 128 ms, inversion time 2,500 ms, flip angle of 180°, matrix size 384 x 384, slice thickness 2 mm. Set the parameters for the 3D-real IR as follows: TR 6,000 ms, TE 155 ms, inversion time 1,500 ms, flip angle 180°, matrix size 320 x 320, slice thickness 0.5 mm.

3. MRI Quality Check and Identification of Endolymphatic Hydrops in MRI

1. Check the MRI image quality with regard to artifacts like fold-over artifacts, pulsation artifacts, metal artifacts, and take special account of the target of evaluation, in this case the cranial nerves VII and VIII throughout their course.
2. Evaluate the endolymphatic hydrops in the MRI-scans of patient group. Check for degree of cochlear and labyrinthine endolymphatic hydrops made visible by examining the acquired 3D-FLAIR- and 3D-real IR-sequences (**Figure 1**).

4. Image Based Measurements of Cranial Nerves

1. **General preparations**
    1. Install a DICOM viewer of choice for image evaluation and measurements on the evaluation workstation, *e.g.*, OsiriX or Horos.
    2. Run the DICOM viewer by double clicking the icon of the application; the database window will be displayed.
    3. Import the patient image data by left-mouse clicking on "File" in the upper dropdown menu, then select "Import" → "Import file". In the file selector, select the patient image data; the patient name and data will be displayed in the database window after successful import. NOTE: Importing of compressed files (*e.g.*,.zip) or uncompressed directories of DICOM files is feasible with the aforementioned DICOM viewers.
    4. In the database window expand the patient image folder by left-clicking onto the triangle symbol on the left side of the patient name. Select the sequence of choice from this folder (here CISS sequence) and double left click on it to open the corresponding image data. The patient image data will be displayed.

2. **Reconstructions of cranial nerves**
Note: Because of the long and not always in-plane course of the nerves from the brain stem through the cerebellopontine angle (CPA) into the acoustic meatus and further to the fundus of the internal auditory canal (IAC), the reconstruction and evaluation of the nerve's diameters and CSAs at different levels is necessary.
    1. Prepare for reconstructing transverse sections at the following locations throughout the course of the cranial nerves to avoid measurement errors derived from oblique slices throughout the course of the nerve, by selecting "3D MPR" in the "3D Viewer" dropdown menu at the top of the screen; the MPR-window will be displayed.
    2. Adjust zoom levels to accommodate for the structures to be reconstructed (here cranial nerves VII and VIII) by selecting the zoom tool (magnifying glass) from the "Change mouse button function" area in the toolbar in the upper left part of the MPR-window. Then move

the mouse cursor to each of the 3 planes in the MPR-window and adjust zoom levels by left click and dragging the mouse (the mouse cursor will transform into a magnifying glass).

3. Reconstruct the central VIII nerve and set the reconstruction plane orthogonal to the nerves course in the middle of the CPA. Check and adapt the orientation of the reconstructed plane in all 3 planes/windows (it should be reconstructed orthogonal to the direction of the crossing of the nerve in order to avoid partial volume effects at the following measurements).
    1. Check for out of plane traversing of the nerve and correct the plane orientation respectively.
        1. To correct plane orientation, move the mouse cursor to the center of the axis crosshair of each plane in the MPR-window (when located correctly the mouse cursor will transform into a hand symbol).
        2. Grab the axis crosshair in each of the 3 planes/windows individually with the grab tool indicated by the hand-icon, and move the axis approximately to the entry to the internal acoustic meatus in each of the 3 planes.
        3. Adjust the orientation of the 3 axes to the nerve's course using the rotate-function available by moving the mouse to the lateral aspects of each axis (the correct rotate-function is depicted by a change of the mouse cursor to a curvilinear icon). Then hold the left mouse button pressed and drag the mouse to adjust the plane orientation.
        4. Adjust the plane orientation in all 3 windows of the MPR-window. In order to reconstruct a plane transverse to the VIII nerves course at the level of the middle of the CPA, go to the left lower window in the MPR-window, and move the mouse to the middle of the axis crosshair so the mouse cursor will transform again into a hand symbol. Then left click and drag the plane (orange line) to the desired location (here, to the middle of the CPA).
        5. Adjust the zoom levels if necessary with the zoom tool (the mouse will change its icon to a magnifying glass) by left clicking and dragging.
        6. Left click into the upper right window of the MPR-window to select this plane. Select "File" → "Export" → "Export to DICOM file(s)". In the "DICOM Export"-window select "Sequence:" → "Current image only" by left clicking into adjacent circle selector.
        7. Rename the series appropriately, here "VIII CPA". Then left click the "OK"-button on the right lower aspect of the DICOM export window.
           NOTE: This will close the DICOM export window, will save the reconstructed image into the patient database, and return to the MPR window.

4. Reconstruct the orthogonal views of the branches of VIII nerve: cochlear nerve (CN), superior vestibular nerve (SVN), and inferior vestibular nerve (IVN) at the level of the meatus of the IAC, where representative visualization is usually well feasible. Check for out of plane traversing of the nerve and correct the plane orientation respectively.
    1. Grab the axis crosshair in each of the 3 planes/windows with the grab tool indicated by a hand-icon, move the axis toward the CN, SVN, and IVN, respectively at the level of the meatus of the IAC, and adjust their orientation to the nerve's course using the rotate-function available at the lateral aspects of each axis depicted by the curved icon, as described under step 4.2.3.1.1 - 4.2.3.1.5.
    2. Export and rename the reconstructed planes as under step 4.2.3.1.6 - 4.2.3.1.7.

5. Reconstruct the orthogonal views of the facial nerve (cranial nerve VII) at the level of the CPA, meatus of the IAC, and fundus of the IAC as described under step 4.2.3. Check for out of plane traversing of the nerve and correct the plane orientation respectively at each level of reconstruction.

3. **Measurements**
Note: Perform the following measurements: measure CSA, long diameter (LD) and perpendicular short diameter (SD) of the facial nerve (cranial nerve VII) and vestibulocochlear nerve (cranial nerve VIII) in the reconstructed transverse images (**Figure 4** and **Figure 5**). Pay attention to consistent windowing levels between scans to avoid partial volume effects influencing the quantificational measurements in a non-systematic way.
    1. Select the previously reconstructed image of cranial nerve VIII at the level of CPA by left clicking the corresponding image file (previously named "VIII CPA") in the database window of the DICOM viewer. Open it by double left-clicking on the filename. The reconstructed image will open in a single window.
    2. Zoom in into the image structures if necessary as instructed at step 4.2.2. Select "Length" by left clicking with the mouse on the triangular symbol next to the "Change the mouse button function" in the toolbar on top of the screen. Left click and hold the left mouse button pressed to draw a line of measurement for the longest diameter of the cranial nerve VIII; this measurement is LD.
    3. Perform a measurement perpendicular to LD for the SD measurement.
       NOTE: The measurements will be automatically stored if using OsiriX or Horos as DCIOM viewer.
        1. Repeat these measurements of LD and SD also in the reconstructions of the VIII nerve at the level of the meatus of the IAC by measuring in the image file from the image database named "VIII meatus" and at the level of the fundus of the IAC, file name "VIII fundus".

    4. Evaluate CSA preferably using the closed polygon region-of-interest (ROI) to account for possible inhomogeneities in the contour of the cranial nerve's cross section. In the toolbar on the upper part of the screen, press the triangular symbol on the right of the "Mouse button function" area and select "Closed Polygon" (the previously selected line symbol will change to a polygon).
    5. Outline the contour of the cranial nerve VIII by left clicking multiple times on the border of the nerve. To close the polygon double left click at the desired point; the complete contour will be displayed.
       Note: If necessary correct the position of the polygon points by left clicking and moving.
    6. Open the previously performed reconstruction of the facial nerve at the level of the CPA (image file name "VII CPA") and perform measurements of LD, SD, and CSA for cranial nerve VII following steps 4.3.1 - 4.3.5.
    7. Open the reconstructions at the level of the meatus of the IAC and perform measurements of LD, SD, and CSA for the CN, SVN, IVN, and cranial nerve VII following steps 4.3.1 - 4.3.5.

8. Open the reconstructions at the level of the fundus of the IAC and perform measurements of LD, SD, and CSA for the CN, SVN, IVN, and cranial nerve VII following steps 4.3.1 - 4.3.5.

Representative Results

Statistical analysis was performed using statistical analysis software, and two-sided independent samples *t*-test was applied. Image evaluation was performed by two readers. A significant difference between the mean values of the patient group (n = 21) and healthy control group (n = 39) can be found for measurements of the CSA of the facial nerve, CN, SVN, and IVN (**Table 2**). CSA measurements in the patient group showed significantly larger CSA values (**Figure 2** and **Figure 3**). Evaluation of measurements of the LD and SD showed varying results, depending on the site of measurement, and differences in LD and SD between the two groups were found. For example, at the level of the meatus, SD of the SVN was significantly larger in the patient group compared to the healthy control group, whereas LD was found to be not significantly different (**Table 3** and **Table 4**). Mediator-based theories of MD support these findings[7,15].

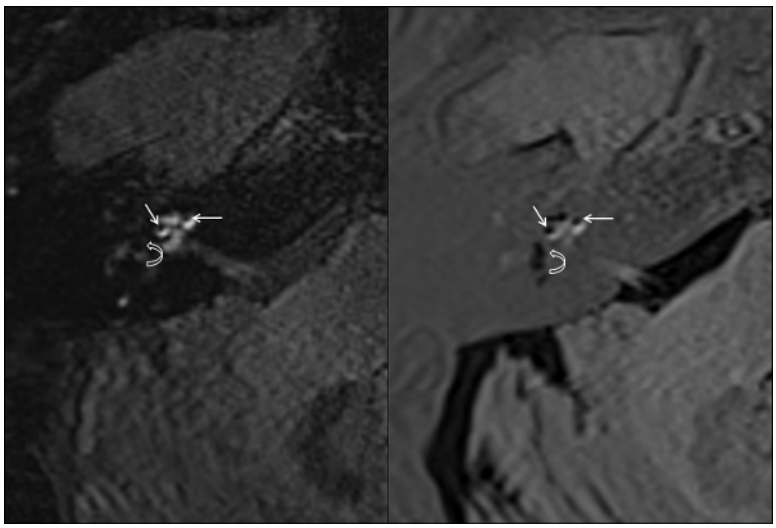

Figure 1: Endolymphatic hydrops in MRI scans. High grade endolymphatic hydrops of the cochlea (straight arrows) and the vestibule (curved arrows) in 3D-FLAIR (**A**) and 3D-Real-IR (**B**). Please click here to view a larger version of this figure.

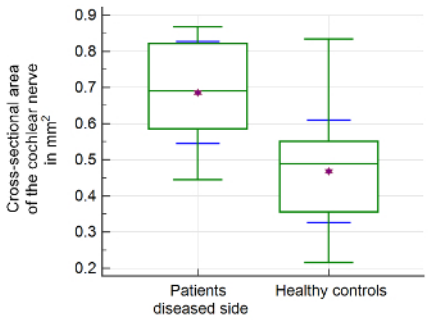

Figure 2: Morphometric evaluation of cochlear nerve. Significant differences of mean values and interquartile ranges of the cross-sectional area (CSA) of the cochlear nerve were found in the patient group compared to healthy controls. The upper and lower green horizontal lines depict minimal and maximal values, connected by the whisker. The purple star shows the arithmetic mean. The green middle line represents the median. The blue error bars depict 1 SD. Please click here to view a larger version of this figure.

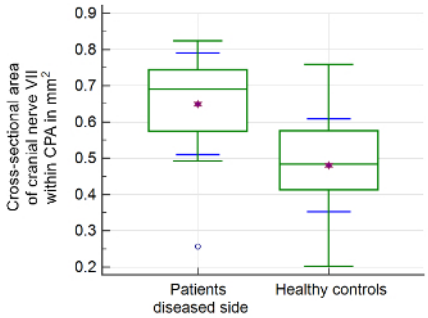

Figure 3: Morphometric evaluation of cranial nerve VII. Significant differences of the cross-sectional area (CSA) of the facial nerve at the level of the cerebellopontine angle (CPA) were found in the patient group compared to healthy controls. The upper and lower green horizontal lines depict minimal and maximal values connected by the whisker. The purple star shows the arithmetic mean. The green middle line represents the median. The blue error bars depict 1 SD. Please click here to view a larger version of this figure.

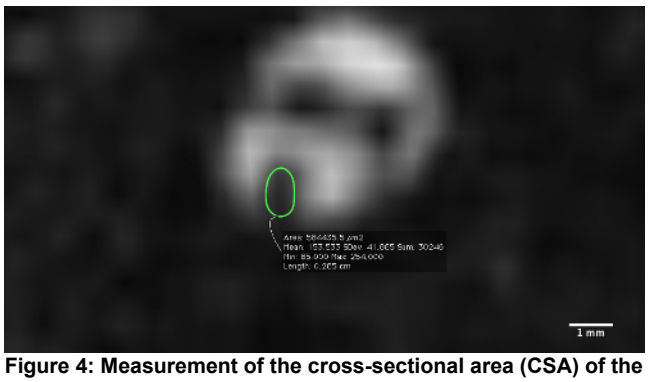

Figure 4: Measurement of the cross-sectional area (CSA) of the cochlear nerve. Measurement performed at the fundus of the internal meatus on a reconstructed slice perpendicular to the nerve's course. Please click here to view a larger version of this figure.

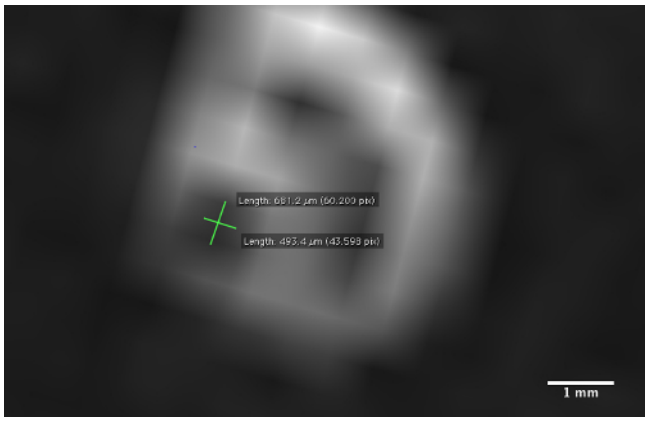

Figure 5: Measurement of the long diameter (LD) and perpendicular short diameter (SD) of the cochlear nerve. Measurement performed at the fundus of the internal meatus on a reconstructed slice perpendicular to the nerve's course. Please click here to view a larger version of this figure.

Mr-sequence parameters	**3D-CISS**
TR	5.79 ms
TE	2.58 ms
Flip angle	34°
Field of view	160 x 160 mm^2
Matrix size	320 x 320
Averages	1
Slice thickness	0.5 mm

Table 1: MRI sequence parameters. Set MRI sequence parameters as described using Constructive Interference in Steady State (CISS)-sequence technique for achieving strongly T2-weighted image contrast for optimal depiction of nerves surrounded by cerebrospinal fluid.

Cross-Sectional Area (mm²)

			unilaterally diseased				all patients (bilaterally diseased)	
nerve	level of measurement	parameter	patients diseased side	healthy controls	patients non-dis. side	healthy controls	patients diseased side	healthy controls
VIII	CPA	mean ± sd	1.33 ± 0.31	1.45 ± 0.35	1.39 ± 0.30	1.45 ± 0.35	1.37 ± 0.30	1.45 ± 0.35
		P	0.2665		0.6166		0.3705	
CN	meatus	mean ± sd	0.69 ± 0.14	0.46 ± 0.14	0.71 ± 0.13	0.46 ± 0.14	0.70 ± 0.12	0.46 ± 0.14
		P	**< 0.0001**		**< 0.0001**		**< 0.0001**	
SVN	meatus	mean ± sd	0.61 ± 0.08	0.40 ± 0.12	0.59 ± 0.08	0.40 ± 0.12	0.62 ± 0.09	0.40 ± 0.12
		P	**< 0.0001**		**< 0.0001**		**< 0.0001**	
IVN	meatus	mean ± sd	0.46 ± 0.12	0.33 ± 0.12	0.53 ± 0.12	0.33 ± 0.12	0.47 ± 0.11	0.33 ± 0.12
		P	0.0008		**< 0.0001**		**< 0.0001**	
VII	CPA	mean ± sd	0.65 ± 0.14	0.48 ± 0.13	0.65 ± 0.09	0.48 ± 0.13	0.67 ± 0.12	0.48 ± 0.13
		P	**0.0001**		**< 0.0001**		**< 0.0001**	
VII	meatus	mean ± sd	0.62 ± 0.13	0.35 ± 0.12	0.64 ± 0.13	0.35 ± 0.12	0.63 ± 0.12	0.35 ± 0.12
		P	**< 0.0001**		**< 0.0001**		**< 0.0001**	
VII	fundus	mean ± sd	0.62 ± 0.13	0.39 ± 0.10	0.64 ± 0.12	0.39 ± 0.10	0.64 ± 0.12	0.39 ± 0.10
		P	**< 0.0001**		**< 0.0001**		**< 0.0001**	

Table 2: Morphometric analysis results of cross-sectional area measurements (CSA). Comparison of patients vs. healthy controls measuring CSA of the 7th and 8th cranial nerve at different levels through their course. Analysis of unilaterally affected patients, bilaterally affected patients, and healthy controls including mean value, standard deviation, and *p*-values (independent samples *t*-test, patient group n = 21, healthy controls n = 39); significant results with $p < 0.000595$ after Bonferroni correction are marked bold.

Long Diameter (mm)

			unilaterally diseased				all patients (bilaterally diseased)	
nerve	level of measurement	parameter	patients diseased side	healthy controls	patients non-dis. side	healthy controls	patients diseased side	healthy controls
VIII	CPA	mean ± sd	1.34 ± 0.24	1.56 ± 0.36	1.43 ± 0.24	1.56 ± 0.36	1.38 ± 0.24	1.56 ± 0.36
		P	0.0281		0.1865		0.0161	
CN	meatus	mean ± sd	0.82 ± 0.11	0.71 ± 0.16	0.83 ± 0.11	0.71 ± 0.16	0.84 ± 0.10	0.71 ± 0.16
		P	0.0192		0.0126		**0.0003**	
SVN	meatus	mean ± sd	0.81 ± 0.11	0.70 ± 0.18	0.83 ± 0.11	0.70 ± 0.18	0.83 ± 0.11	0.70 ± 0.18
		P	0.0118		0.0154		0.0027	
IVN	meatus	mean ± sd	0.68 ± 0.11	0.65 ± 0.17	0.75 ± 0.08	0.65 ± 0.17	0.70 ± 0.11	0.65 ± 0.17
		P	0.5249		0.0076		0.1748	
VII	CPA	mean ± sd	0.80 ± 0.12	0.71 ± 0.16	0.82 ± 0.09	0.71 ± 0.16	0.83 ± 0.12	0.71 ± 0.16
		P	0.0467		0.0022		0.0021	
VII	meatus	mean ± sd	0.86 ± 0.08	0.65 ± 0.20	0.83 ± 0.11	0.65 ± 0.20	0.87 ± 0.09	0.65 ± 0.20
		P	**< 0.0001**		**0.0002**		**< 0.0001**	
VII	fundus	mean ± sd	0.79 ± 0.07	0.72 ± 0.14	0.82 ± 0.12	0.72 ± 0.14	0.84 ± 0.09	0.72 ± 0.14
		P	0.018		0.0183		0.0007	

Table 3: Morphometric analysis results of long diameter (LD). Comparison of patients vs. healthy controls measuring LD of the 7th and 8th cranial nerve at different levels through their course. Analysis of unilaterally affected patients, bilaterally affected patients, and healthy controls including mean value, standard deviation, and *p*-values (independent samples *t*-test, patient group n = 21, healthy controls n = 39).

Short Diameter (mm)

			unilaterally diseased				all patients (bilaterally diseased)	
nerve	level of measurement	parameter	patients diseased side	healthy controls	patients non-dis. side	healthy controls	patients diseased side	healthy controls
VIII	CPA	mean ± sd	0.86 ± 0.16	0.78 ± 0.14	0.85 ± 0.17	0.78 ± 0.14	0.85 ± 0.14	0.78 ± 0.14
		P	0.1195		0.1929		0.0905	
CN	meatus	mean ± sd	0.60 ± 0.10	0.49 ± 0.09	0.62 ± 0.07	0.49 ± 0.09	0.58 ± 0.09	0.49 ± 0.09
		P	**0.0002**		**< 0.0001**		**0.0003**	
SVN	meatus	mean ± sd	0.53 ± 0.08	0.41 ± 0.07	0.51 ± 0.06	0.41 ± 0.07	0.53 ± 0.09	0.41 ± 0.07
		P	**< 0.0001**		**< 0.0001**		**< 0.0001**	
IVN	meatus	mean ± sd	0.48 ± 0.08	0.37 ± 0.09	0.49 ± 0.09	0.37 ± 0.09	0.46 ± 0.09	0.37 ± 0.09
		P	**0.0003**		**0.0003**		**0.0004**	
VII	CPA	mean ± sd	0.57 ± 0.14	0.50 ± 1.13	0.50 ± 0.12	0.50 ± 0.13	0.58 ± 0.13	0.50 ± 0.13
		P	0.125		0.9758		0.0265	
VII	meatus	mean ± sd	0.52 ± 0.11	0.39 ± 0.09	0.53 ± 0.10	0.39 ± 0.09	0.53 ± 0.11	0.39 ± 0.09
		P	**0.0001**		**< 0.0001**		**< 0.0001**	
VII	fundus	mean ± sd	0.53 ± 0.11	0.39 ± 0.07	0.53 ± 0.08	0.39 ± 0.07	0.53 ± 0.10	0.39 ± 0.07
		P	**0.0002**		**< 0.0001**		**< 0.0001**	

Table 4: Morphometric analysis results of short diameter (SD). Comparison of patients vs. healthy controls measuring SD of the 7th and 8th cranial nerve at different levels through their course. Analysis of unilaterally affected patients, bilaterally affected patients, and healthy controls including mean value, standard deviation, and *p*-values (independent samples *t*-test, patient group n = 21, healthy controls n = 39).

Discussion

We have demonstrated a feasible and accessible method of evaluation of morphometric changes of cranial nerves, as they may occur in several pathophysiological situations, here in MD compared to normal hearing controls.

Modifications and Troubleshooting:

Similar measurements to the ones reported here for the 7th and 8th cranial nerves can be performed using the employed 3D-CISS-sequence scans for all other cranial nerves at different levels, as long as they are still surrounded by cerebral fluid, otherwise contrast issues may arise with the mentioned MR-scanning sequence technique. For morphometric analysis of cranial nerves at levels where they are not surrounded by liquid, changes of the MR scanning protocol become mandatory, *e.g.*, application of intravenous Gadolinium or employment of MRI fat-suppression techniques. Measurements in orthogonal reconstructions throughout the nerves course remain mandatory.

When combining MR-based evaluation of endolymphatic hydrops with morphometric analysis, the MR-scan can not only be used for describing anatomical changes of cranial nerves but can also aid in the diagnosis of MD. In the future, automated morphometric analysis techniques including machine based learning and artificial intelligence may speed up the evaluation and improve consistency of measurements and evaluations.

In a general approach for morphometric analysis of cranial nerves, MRI examinations can be performed "natively" without the use of intravenous or intratympanic administration of MRI contrast agents. In the protocol diluted intratympanic contrast agent has been applied in order to quantify the severity of endolymphatic hydrops occurring in MD, relevant for the diagnosis of the disease. The small amount and small concentration of Gadolinium-based contrast agent via intratympanic application in this study does not show effects on quantitative measurements of signal intensities of cerebrospinal fluid or the nerves when comparing the diseased side and contralateral side in MD patients, a finding corroborated by other studies. Signal intensities, image quality, and contrast do not differ when comparing strongly T2-weighted images of Gadolinium-injected patients with images of the non-injected controls[16]. Therefore, the effects of the contrast agent on the morphometric measurements do not play a role. Until today no evidence was found that Gadolinium might play a role on brain or cranial nerves with regard to alterations of volume. However, the long-term effects of Gadolinium-based contrast agents on cranial nerves remains to be studied. Intratympanic application of Gadolinium in healthy controls remains unethical and therefore wasn't performed in the normal hearing patients in this study.

Future Applications:

The depicted method allows for comparison of morphometric changes of cranial nerves in a very large variety of diseases and in several neural structures. Future transfer of the method for evaluating morphometric changes of cranial nerves *e.g.*, in chronic pain, Alzheimer's Disease, or multiple sclerosis (MS) and comparing those findings to healthy controls is feasible.

Critical Steps Within the Protocol and Limitations of the Technique:

When evaluating morphometric parameters using the described techniques, set consistent windowing levels throughout the scans and/or let the measurements be performed by two or more readers. To avoid inter-rater variability, let each reader evaluate all scans. Using thin slice thickness and slice orientation perpendicular to the course of the cranial nerves is mandatory, throughout the whole course of the nerves. When comparing different studies performed on different MR-scanners, it must be considered that differences in MR scan parameters can result in differences in partial volume effects, as well as differences with regard to image contrasts and image quality. The levels at which morphometric analysis throughout the course of the cranial nerves was performed in different studies need to be considered when comparing studies.

Disclosures

The authors have nothing to disclose.

Acknowledgements

Robert Gürkov received fundings from the German Ministry of Research and Education BMBF, Grant No. 01 EO 0901.

References

1. Gurkov, R. *et al.* In vivo visualized endolymphatic hydrops and inner ear functions in patients with electrocochleographically confirmed Meniere's disease. *Otol Neurotol.* **33** (6), 1040-1045 (2012).
2. Gurkov, R., Flatz, W., Louza, J., Strupp, M., & Krause, E. In vivo visualization of endolyphatic hydrops in patients with Meniere's disease: correlation with audiovestibular function. *Eur Arch Otorhinolaryngol.* **268** (12), 1743-1748 (2011).
3. Gurkov, R., Pyyko, I., Zou, J., & Kentala, E. What is Meniere's disease? A contemporary re-evaluation of endolymphatic hydrops. *J Neurol.* **263 Suppl 1** S71-81 (2016).
4. Plontke, S. K., & Gurkov, R. [Meniere's Disease]. *Laryngorhinootologie.* **94** (8), 530-554 (2015).
5. Klockars, T., & Kentala, E. Inheritance of Meniere's disease in the Finnish population. *Arch Otolaryngol Head Neck Surg.* **133** (1), 73-77 (2007).
6. Greco, A. *et al.* Meniere's disease might be an autoimmune condition? *Autoimmun Rev.* **11** (10), 731-738 (2012).
7. Ozdogmus, O. *et al.* Connections between the facial, vestibular and cochlear nerve bundles within the internal auditory canal. *J Anat.* **205** (1), 65-75 (2004).
8. Nakamichi, R. *et al.* Establishing normal diameter range of the cochlear and facial nerves with 3D-CISS at 3T. *Magn Reson Med Sci.* **12** (4), 241-247 (2013).
9. Kang, W. S. *et al.* Normative diameters and effects of aging on the cochlear and facial nerves in normal-hearing Korean ears using 3.0-tesla magnetic resonance imaging. *Laryngoscope.* **122** (5), 1109-1114 (2012).
10. Jaryszak, E. M., Patel, N. A., Camp, M., Mancuso, A. A., & Antonelli, P. J. Cochlear nerve diameter in normal hearing ears using high-resolution magnetic resonance imaging. *Laryngoscope.* **119** (10), 2042-2045 (2009).
11. Henneberger, A., Ertl-Wagner, B., Reiser, M., Gurkov, R., & Flatz, W. Morphometric evaluation of facial and vestibulocochlear nerves using magnetic resonance imaging: comparison of Meniere's disease ears with normal hearing ears. *Eur Arch Otorhinolaryngol.* **274** (8), 3029-3039 (2017).

12. Zwergal, A., Brandt, T., Magnusson, M., & Kennard, C. DIZZYNET: the European network for vertigo and balance research. *J Neurol.* **263 Suppl 1** S1 (2016).
13. Zwergal, A., Brandt, T., Magnusson, M., & Kennard, C. DIZZYNET--a European network initiative for vertigo and balance research: visions and aims. *J Neurol.* **263 Suppl 1** S2-9 (2016).
14. Grill, E. *et al.* DizzyReg: the prospective patient registry of the German Center for Vertigo and Balance Disorders. *J Neurol.* (2017).
15. Semaan, M. T., Alagramam, K. N., & Megerian, C. A. The basic science of Meniere's disease and endolymphatic hydrops. *Curr Opin Otolaryngol Head Neck Surg.* **13** (5), 301-307 (2005).
16. Hayashi, M. *et al.* Usefulness of the advanced neuroimaging protocol based on plain and gadolinium-enhanced constructive interference in steady state images for gamma knife radiosurgery and planning microsurgical procedures for skull base tumors. *Acta Neurochir Suppl.* **116** 167-178 (2013).

